Journal of Quantitative Spectroscopy & Radiative Transfer 242 (2020) 106757

Contents lists available at ScienceDirect

Journal of Quantitative Spectroscopy & Radiative Transfer

journal homepage: www.elsevier.com/locate/jqsrt

# A light-scattering study of highly refractive, irregularly shaped $MoS_2$ particles

Prakash Gautam, Christopher M. Sorensen*

*Department of Physics, Kansas State University, Manhattan, KS 66506, USA*

ARTICLE INFO

*Article history:*
Received 22 August 2019
Revised 6 November 2019
Accepted 12 November 2019
Available online 13 November 2019

*Keywords:*
Light scattering
irregular particles
Complex refractive index
Mie theory
Optical particle sizing

ABSTRACT

We present measurements of light scattering intensity from aerosolized, micron sized, irregularly shaped, molybdenum disulfide ($MoS_2$) particles in order to study the effects of a refractive index, $m = n + i\kappa$, with large real and imaginary parts. Light scattering was measured over a range of angles from 0.32° to 157°. Calibration was achieved by scattering with micron sized, spherical silica particles. Light scattering for both particle types was compared to theoretical Mie scattering calculations using size distributions determined by an aerodynamic particle sizer. Effects of the intensity weighted size distribution are discussed. We find that scattering by these irregularly shaped, highly refractive particles is well described by Mie scattering. We also find that when the quantity $\kappa kR$, where $kR = 2\pi R/\lambda$ is the size parameter, is greater than one, there is no enhancement in the backscattering. Finally, we show that Guinier analysis of light scattering by highly refractive particles yields intensity weighted mean sizes of reasonable accuracy for any shape.



## 1. Introduction

In recent work we have explored the light scattering properties of micron sized, irregularly shaped particles as reviewed in [1], and in particular from a Q-space point of view (see below). Part of our program has been experimental measurement of the angular distribution of the scattered light from aerosolized Arizona road dust [2] and $Al_2O_3$ abrasive particles [3]. An important characteristic of our scattering studies is that they have been carried out over a broad range of angles including very small angles necessary for proper characterization of large particles. Here we present a similar study of aerosolized, micron sized, irregularly shaped, molybdenum disulfide ($MoS_2$) particles. We choose this material because it has rather extreme values of the real and imaginary parts of the refractive index, hence expands the phase space of independent variables that control scattering that we have so far explored. Furthermore, the important practical reason for all our work is that these particle types are common in the atmosphere, typically as dusts, and their light scattering and absorption properties play a significant role in the Earth's radiation budget. Radiative forcing calculations generally rely on Mie theory which is rigorous for spherical particles only [4,5]. Our work allows us to investigate questions that arise regarding the nature of light scattering by highly refractive and absorptive irregularly shaped particles and how well Mie theory describes the scattering.

The complex refractive index for $MoS_2$ has been reported as $m = n + i\kappa = 5.24 + i1.16$ [6], $4.43 + i1.17$ [7] and $4.41 + i0.63$ [8] for the wavelength $\lambda = 532$ nm. We used a commercially available aerodynamic particle sizer spectrometer (APS 3321 (TSI)) to determine the size distribution of the aerosolized $MoS_2$ particles from which we scattered light. With this, we calculated the scattering using the Mie equations and compared that to the scattering data with some success. This analysis highlights the problems of an intensity weighted size distribution. In addition, we studied backscattering and showed that when the imaginary part of the refractive index $\kappa$ is large compared to the inverse of the size parameter, $(2\pi R/\lambda)^{-1}$, where R is the effective particle radius and $\lambda$ is the optical wave length; there is no enhancement in the backscattering.

We applied Q-space analysis [1,9,10] to the experimentally observed results. Q-space analysis is the double logarithmic plotting of the scattered intensity versus the magnitude of the scattering wave vector, q, rather than the conventional linear angle. The magnitude of the scattering wave vector is given by

$$q = 2\ k\ \sin(\theta/2), \tag{1}$$

where $k = 2\pi/\lambda$, $\lambda$ is the wavelength of light used and $\theta$ is the scattering angle. Further, the Q-space plot facilitates Guinier analysis which yields a measure of the size of the scatterer [11,12].

* Corresponding author.
*E-mail address:* sor@phys.ksu.edu (C.M. Sorensen).

https://doi.org/10.1016/j.jqsrt.2019.106757
0022-4073/

## 2. Experimental method

An extensive description for the light scattering experimental setup can be found in Wang et al. [2]. Briefly, two 16 channel photodiode detectors *viz*. a forward detector and a side detector, collected the scattered light at a total of 31 different angles. The remaining channel of the side detector was sacrificed to the monitor. The forward alignment is based on the design by Ferri [13]. The forward scattering angle ranges from 0.32° to 9.9°.

For the side scattering, an elliptical mirror was used to collect the scattered light and focus it onto the side detector. The side scattering angle ranged from 15° to 157°. The forward and side detectors were calibrated to each other as described in [2]. The light source was a laser operating at $\lambda = 532$ nm linearly polarized perpendicular to the scattering plane. Use of incident light polarized perpendicular to the scattering plane insures that any functionality on scattering angle, hence q, is not due to the incident polarization but is related to the nature of the scattering particles. Our apparatus covers a wide range of scattering angles from 0.32° to 157° thereby yielding the magnitude of scattering wave vector (q) from 660 $cm^{-1}$ to 2.3 $\times$ $10^5$ $cm^{-1}$.

To aerosolize the particles we used a lab-made dust generator. An aerodynamic particle sizer (APS 3321) has been used to measure the particle number size distributions. The APS 3321 had been calibrated by the manufacturer within 9 months prior to this experiment. Note that manufacturer recommends the APS 3321 be calibrated every 3 years. APS sheath and the aerosol flow rate were measured to be 4 $\pm$ 0.07 lpm and 1 $\pm$ 0.04 lpm, respectively. This is well within the range recommend by TSI. For analyzing the sizing accuracy of APS 3321, we used two different sizes of NIST traceable monodisperse polystyrene latex (PSL) spherical particles with manufacturer reported certified mean diameters 0.994 μm $\pm$ 0.021 μm and 6.15 μm $\pm$ 0.045 μm from Thermo Fisher Scientific, Waltham, MA, USA. We aerosolized PSL spheres using a nebulizer in combination with an aerosol diffusion dryer filled with silica gel as an absorbing agent. The APS measured sizes were found to be 0.98 $\pm$ 0.03 μm and 5.88 $\pm$ 0.1 μm, respectively. The differences between the manufacturer reported and the APS measured values are relatively minor to imply that our APS 3321 is measuring the particle size distribution correctly.

We calibrated the APS results with the light scattering by studying spherical silica ($SiO_2$) particles bought from US Research Nanomaterials, Inc. We did not scatter from PSL due to a low signal/noise ratio. The high sphericity of the silica particles makes them trustworthy subjects of the Mie calculations made for their measured size distribution; thus they provide our benchmark for connecting the APS measured size distribution, the light scattering and the Mie calculations made with the APS data. After calibrating our whole experimental system, we investigated the light scattering due to irregular molybdenum disulfide ($MoS_2$) particles.

A TEM and an optical microscope were used to determine additional particle size and shape information. A theoretical Mie calculation of the scattering spectrum using the size distribution from APS and optical constant from prior published literature is compared to the light scattering result. We apply Guinier analysis to test the consistency of the size measurement by light scattering with microscopy.

## 3. Results

### 3.1. Calibration of APS 3321 measurements with light scattering

The manufacturer reported mean diameter for the silica particle is 0.82 μm. The size distribution of aerosolized silica was measured by the APS. The aerosol was collected at the light scattering volume. The volume equivalent sphere diameter is required for the Mie calculation. However, the APS instead measured the aerodynamic diameter. The volume equivalent diameter ($D_v$) is related to the aerodynamic diameter ($D_a$) by [14,15]

$$D_v = D_a \sqrt{\frac{\chi \rho_0}{\rho_p}} \tag{2}$$

where $\rho_0$ is the unit density (1 g /cc), $\rho_p$ is the particle density and $\chi$ is the aerodynamic shape factor of the particle. The aerodynamic shape factor is the ratio of drag force acting on a non-spherical particle to that of a spherical particle of having the same volume and settling velocity (for a sphere, $\chi = 1$). For Eq. (2), we used $\chi = 1$ because the TEM pictures shown in Fig. 1 indicate that the particles are spherical in shape. Fig. 2 shows the volume equivalent particle number distribution for the $SiO_2$ aerosol and their transformed light scattering intensity weighted distribution. The contribution of each particle in this weighted distribution will be proportional to the $D^4$, and the reasons for this weighting will be described below.

The volume equivalent particle number size distribution peaks at a diameter of 1.11 μm, and we used the corresponding radius for Mie calculations. The geometric standard deviation for this distribution was found to be $\sigma = 1.58$. With $\lambda = 532$ nm, the size

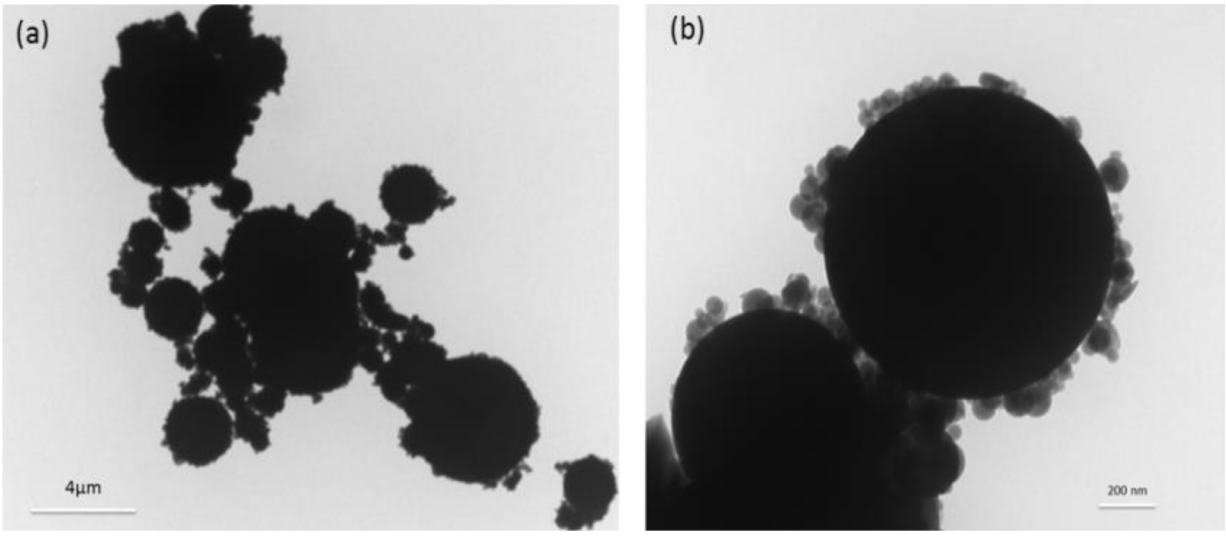


**Fig. 1.** Transmission electron microscope images for silica ($SiO_2$) particles

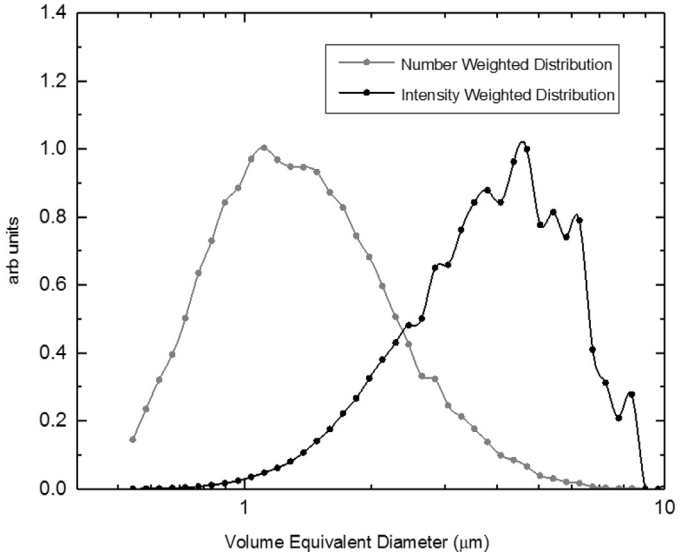


**Fig. 2.** Particle number distribution for the silica ($SiO_2$) particles measured with the APS 3321 after converting aerodynamic diameter ($D_a$) to the volume equivalent diameter ($D_v$) and its transformation to an intensity weighted distribution with a weighting factor of $D^4$ .

parameter for the peak size is given by kR = 6.5. The refractive index for the silica particles is taken to be $m = n + i\kappa = 1.46 + i0$ at $\lambda = 532$ nm [16]. With these parameters, the Mie calculations were performed and then compared to our experimental result as shown in Fig. 3.

Fig. 3 shows that at a small angle range, the Mie calculation and the data agree excellently. This angle range is least sensitive to the particle non-sphericity and its optical constants. Further, Mie calculations underestimate the light scattering by a factor of $\approx$ 1.48 at angles around 125°. Note that the scattering in this region is about three orders of magnitude smaller than in the forward regime, hence prone to some uncertainty. Jaggard et al. [17] and Mishchenko et al., [18] showed a similar result when comparing Mie calculations for spheres and T – matrix calculations for spheroidal particles. The difference observed in our compared result may be due to nano-size silica attaching to the micron size silica particles (see in Fig. 1) thereby creating a distortion in sphericity. Overall, the Mie calculation for APS 3321 observed data agrees quite well with the experimental result.

The Q-space plot shows a constant forward scattering lobe at smallest q. This is followed by a Guinier regime near $q \simeq R^{-1}$ where the q, hence angular, functionality begins. After that, there is a power law regime followed by a small dip that ends with enhanced backscattering. All this is typical of scattering from a polydisperse ensemble of spheres. From the Q-space plot one can determine the radius of gyration, $R_g$, of any arbitrarily shaped particle via Guinier analysis [11] under the assumption of weak refractivity. The Guinier inferred radius of gyration is given by the following equation

$$I(q) = I(0)\left(1 - \frac{q^2 {R_g}^2}{3}\right) \tag{3}$$

where I(q) is the scattering intensity, I(0) is the forward scattering intensity and q is the magnitude of the scattering wave vector, Eq. (1). In principle Guinier analysis is applicable for $qR_g < 1$. But, one can exceed this limit with minor error [19]. When $qR_g$ is small, Eq. (3) can be written as

$$\frac{I(0)}{I(q)} = 1 + \frac{q^2 {R_g}^2}{3} \tag{4}$$

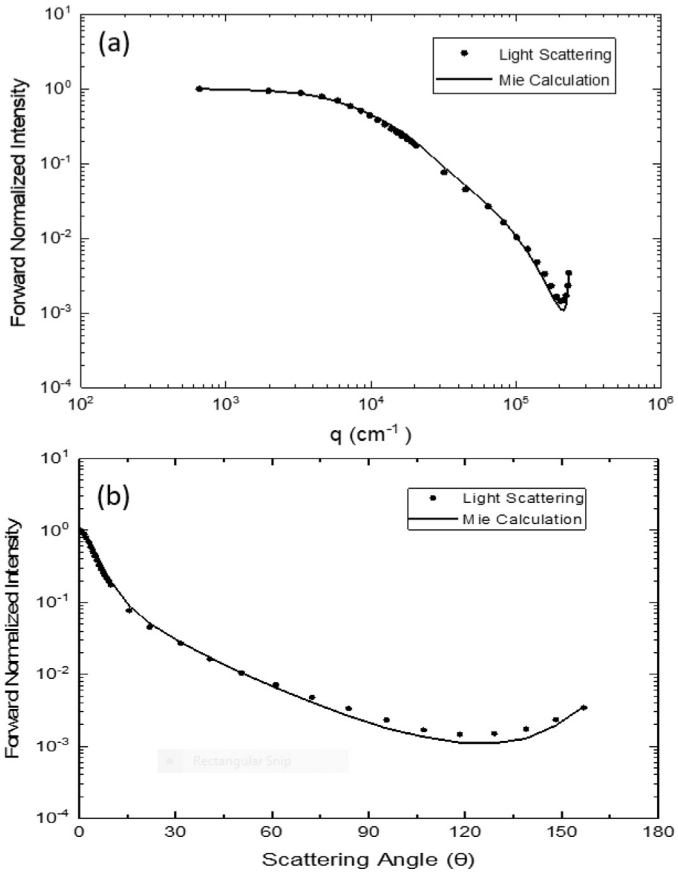


**Fig. 3.** Comparison of the experimentally observed forward normalized light scattering data with Mie calculations for APS observed silica ($SiO_2$) particle size distributions (a) plotted logarithmically versus q, the method of Q-space analysis, and (b) plotted linearly as a function of scattering angle, $\theta$.

We performed the Guinier analysis for our experimentally observed result by plotting the inverse normalized intensity i.e. I(0)/I(q) versus $q^2$ shown in Fig. 4. Eq. (4) indicates that the Guinier plot should be a straight line with slope equal to ${R_g}^2/3$.

We find a measured radius of gyration of $R_g$ = 1.9 μm. This suggests a sphere of radius $R = \sqrt{5/3}R_g = 1.29 \times 1.9 = 2.45\,\mu m$, with a corresponding light scattering inferred diameter of D = 4.9 μm. TEM pictures shown in Fig. 1 indicate a broad size

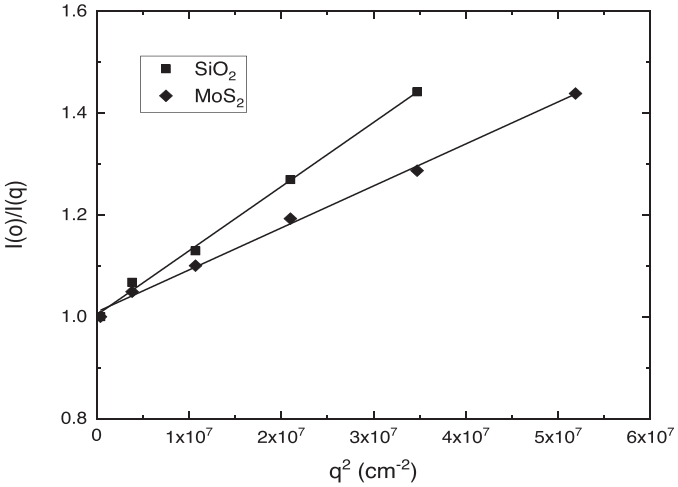


**Fig. 4.** Guinier Analysis of silica ($SiO_2$) particles (squares) and $MoS_2$ particles (diamonds).

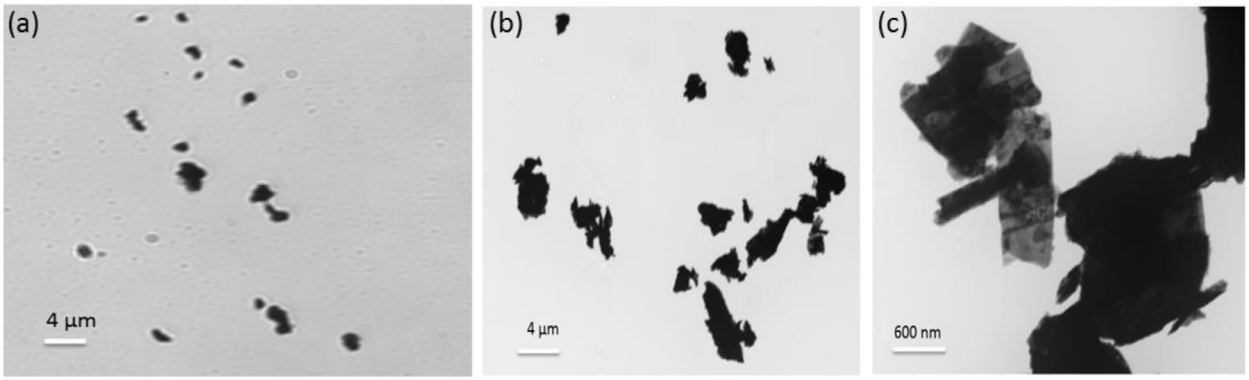


**Fig. 5.** The images of molybdenum disulfide ($MoS_2$) particles: (a) under an optical microscope and (b) and (c) under a transmission electron microscope (TEM).

distribution of particles extending from the nanometer (e.g. 20 nm) range to the micron range. Micron size particles were measured to be around 1–6 μm, which is consistent with the light scattering inferred size because nanometer size particles contribute negligibly to the light scattering in comparison to the micron size particles. More relevant is the APS observed most probable diameter because it sampled the aerosol at the optical scattering volume which was D = 1.11 μm, which is in poor agreement with the light scattering, Guinier size. However, one must realize that light scattering favors the larger sizes of a distribution. The Guinier regime is in the forward scattering regime of the particulate scattering. In this regime, the scattering is proportional to the diameter to the fourth power, i.e. $D^4$ [10,20]. To account for this the APS size distribution is multiplied by $D^4$ and then normalized to have a peak value of unity. This light scattering weighted size distribution is also plotted in Fig. 2. The results are dramatic (although perhaps not surprising). The minor large size tail of the size distribution is emphasized and dominant while the most probable size at D = 1.11 μm is nearly inconsequential. The middle of the light scattering weighted distribution is between 4 and 5 μm, completely consistent with the Guinier inferred size.

The Guinier analysis comes with the caveat that it is accurate only in the diffraction limit when the phase shift parameter $\rho = 2kR|m-1| < 1$, i.e. weakly refractive particles. We have shown [12] that the Guinier inferred radius of gyration, which was designated as $R_{g,G}$, is as much as 50% larger than the true radius of gyration when the phase shift parameter $\rho = 2kR|m-1| > 1$, and 12 % larger in the $\rho \gg 1$ limit.

We conclude by recognizing the semi-quantitative nature of our analysis. However, a good measurement with known caveats is better than no measurement at all. The major caveat here is the heavy weighting of light scattering in favor of the larger particles of a distribution. Moreover, there is considerable uncertainty in the large size tail of the measured distribution because only a small fraction of the particles are there. This weighting is of upmost importance when comparing light scattering measurements to measurements made by the APS and similar devices, and will be important in our analysis below.

### 3.2. Light scattering results for molybdenum disulfide ($MoS_2$) particles

After calibrating with $SiO_2$, we carried out the light scattering experiment for the $MoS_2$ particles. The $MoS_2$ particles were also bought from US Research Nano-Materials, Inc. The size distribution of $MoS_2$ was measured by the APS. Additionally, we used a TEM and an optical microscope to have more insight into particle shape and size. The TEM and optical pictures are shown in the Fig. 5.

The measured aerodynamic diameters were converted to the volume equivalent diameters by using Eq. (2). Our $MoS_2$ particles look like Illite particles which have $\chi = 1.3$ [21]. So, we used a shape factor $\chi = 1.3$ in Eq. (2). Note that with the square root dependence for $\chi$ in Eq. (2), and the fact that $\chi$ is near unity for most shapes, uncertainties in $\chi$ are not significant for our work. Fig. 6 shows the volume equivalent particle number distribution for $MoS_2$ and their transformed light scattering intensity weighted distribution. The number weighted distribution peaks around the diameter 1.13 ± 0.10 μm with geometric standard deviation spread of $\sigma = 1.6$. The size parameter corresponding to this diameter is given by kR = 6.67.

The particle number distribution in Fig. 6 was used for Mie calculations with a refractive index of $m = n + i\kappa = 5.24 + i1.16$ [6]. Using other reported values of m did not change calculations at small angles even though the imaginary refractive index $\kappa$ differs by a factor of two across these values. However, we see a slight difference at larger angles. We have shown [22,23] that effects of $\kappa$ are effectively described by the parameter, $\kappa$kR, the product of the imaginary part of the refractive index and the size parameter. When $\kappa kR \gtrsim 0.1$, $\kappa$ starts to affect the scattering. Once the $\kappa kR \geq 3$, the effect of $\kappa$ saturates. For all reported m, $\kappa kR > 3$; thus, the choice between reported refractive indices is of small consequence for our calculations.

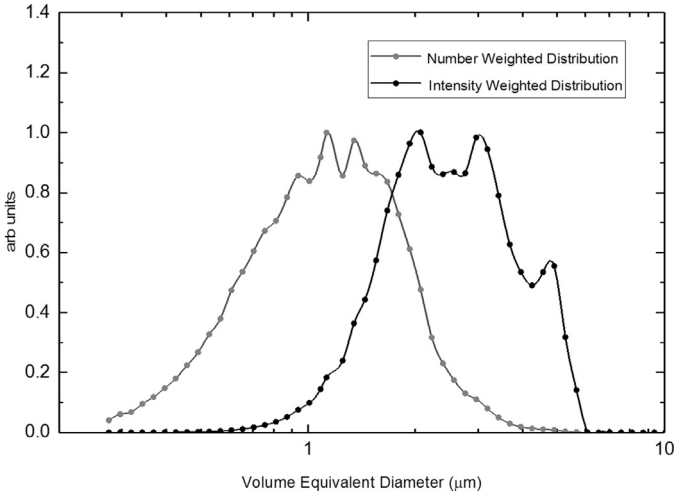


**Fig. 6.** Particle number distribution for the molybdenum disulfide ($MoS_2$) particles measured with the APS 3321 after converting aerodynamic diameter $D_a$ to the volume equivalent diameter $D_v$ and its transformation to an intensity weighted distribution with a weighting factor of $D^4$ .

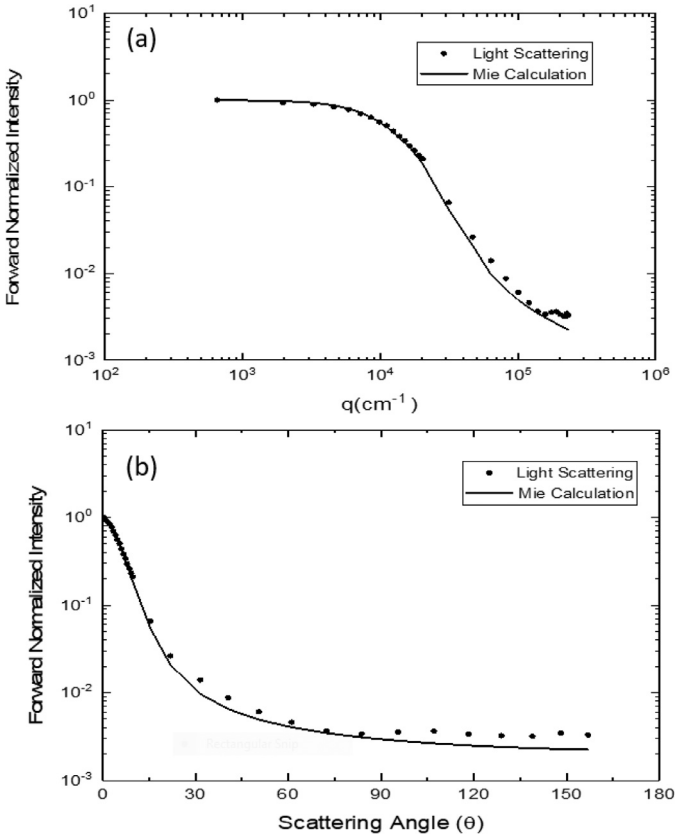


**Fig. 7.** Comparison of the experimentally observed forward normalized light scattering data with Mie calculations for APS observed molybdenum disulfide ($MoS_2$) particle size distributions (a) plotted logarithmically versus q, the method of Q-space analysis and (b) plotted linearly as a function of scattering angle ($\theta$).

Fig. 7 shows a comparison between Mie calculations and experimental results, plotted in Q-space (a) and the more conventional $\theta$-space (b). The Q-space plot shows a forward scattering lobe and a Guinier regime, as for the spherical $SiO_2$ particles, but the subsequent power law regime is ill defined and there is no dip or enhanced backscattering. The conventional plot portrays more clearly the trend of the data in the larger scattering angle range. There is a close agreement between calculation and experiment in the small angle range, but the Mie result slightly underestimates the scattering at larger angles. Here it is valuable to recognize that when the parameter $\kappa$kR is large, essentially all the light scattered energy is in the forward scattering regime [24]. With this perspective, we conclude that Mie theory successfully, but not exactly, describes the scattering, suggesting that the asphericity is rather insignificant for particles having a high refractive index.

Fig. 7 also shows that there is no enhancement in the backscattering up to 157°. This is consistent with the theoretical result of Wang et al. [22] for spheres when $\kappa$kR > 3. For our $MoS_2$ particles we find below an intensity weighted diameter of D = 3.3 μm, hence $\kappa$kR in the range of 12.5–22.75, depending on which of the three reported values of $\kappa$ are used. These are very large values well in the saturated regime where no enhanced backscattering occurs. This result is in contrast to our previous work with irregularly shaped Arizona road dust [2] and abrasive, $Al_2O_3$ particles [3] that had significant enhanced backscattering but had small values of $\kappa$kR.

Finally, the Q-space plot of Fig. 7 shows only a vague power law with q beyond the Guinier regime. This is in contrast to the results for Arizona road dust [2] which showed a strong power law for ~ 1.5 orders of magnitude and the great many examples from the Amsterdam-Granada data set with our re-analysis [25,26]. On the other hand, the $Al_2O_3$ abrasive particles showed only an ill-defined power law. We conclude that the issue of under what circumstances power laws in Q-space occur is uncertain.

Based on the Q-space plot, we apply Guinier analysis on $MoS_2$ data. Fig. 4 includes the Guinier analysis, I(0)/I(q) versus $q^2$ for $MoS_2$. The Guinier analysis shows the radius of gyration $R_g$ to be 1.51 μm. By multiplying $R_g$ by $\sqrt{5/3}$, the three dimensional object equivalent radius becomes R = 1.9 μm. Thus, the light scattering determined diameter is D = 3.8 μm. This result is analogous to the results above for the $SiO_2$ particles. The Guinier inferred size is not seen in the APS number distribution. On the other hand the Guinier inferred size is consistent with the intensity weighted distribution which is in the range D = 2–4 μm. However, as described above, the Guinier inferred radius of gyration is as much as 50% larger than true radius of gyration when the $\rho > 1$ [12]. For our $MoS_2$ at 532 nm, $\rho \approx 55$. At that value, $R_{g,G}$ is greater than $R_g$ by around 12%. Reducing D = 3.8 μm by 12% leads to D = 3.3 μm, which is quite consistent with the sizes given by microscopic pictures in Fig. 5 and the intensity weighted distribution in Fig. 6.

It is useful to look at these Guinier result from the perspective that the Guinier equation was derived for X-ray scattering, and X-rays have a refractive index of essentially one. Indeed, X-ray scattering is simply wave diffraction, the electromagnetic character is insignificant. Nevertheless, our results here show that the Guinier equation applied to light scattering from micron size, highly refractive particles still yields a valuable measure of the size, especially when one considers the difficulties in size measurements by other techniques.

## 4. Conclusion

This experimental study showed that Mie calculations describe light scattering intensity quite accurately for highly refractive, irregular particles. We found that enhanced backscattering (to ≤157°) is not present when the parameter $\kappa$kR is large, a result anticipated by theory. We demonstrated a good connection between light scattering and the size distribution of the aerosolized particles as measured by the aerodynamic particle sizer spectrometer. This connection showed that Guinier analysis of light scattering yields intensity weighted mean sizes of reasonable accuracy for any shape and refractive index. This work also highlighted the rather sever implications of an intensity weighting of the size distribution.

## Declaration of Competing Interest

Professor C. M. Sorensen and Mr. P. Gautum have no conflicts of interest regarding the manuscript: A light-scattering study of highly refractive, irregularly shaped $MoS_2$ particles, by Prakash Gautam and Christopher M. Sorensen.

## Acknowledgment

This work is supported by the National Science Foundation under Grant no. AGM 1649783.

## References

[1] Sorensen CM, Heinson YW, Heinson WR, Maughan JB, Chakrabarti A. Q-space analysis of the light scattering phase function of particles with any shape. Atmosphere 2017;8.
[2] Wang Y, Chakrabarti A, Sorensen CM. A light-scattering study of the scattering matrix elements of Arizona Road Dust. J Quant Spectrosc Radiat 2015;163:72–9.
[3] Heinson YW, Chakrabarti A, Sorensen CM. A light-scattering study of $Al_2O_3$ abrasives of various grit sizes. J Quant Spectrosc Radiat 2016;180:84–91.
[4] van de Hulst HC. Light scattering by small particles. New York: Wiley; 1957.

[5] Bohren CF, Huffman DR. Absorption and scattering of light by small particles. New York: Wiley; 1983.
[6] Beal AR, Hughes HP. Kramers-Kronig Analysis of the Reflectivity Spectra of 2h–Mos2, 2h-Mose2 and 2h-Mote2. J Phys C Solid State 1979;12:881–90.
[7] Yim CY, O'Brien M, McEvoy N, Winters S, Mirza I, Lunney JG, Duesberg GS. Investigation of the optical properties of $MoS_2$ thin films using spectroscopic ellipsometry. Appl Phys Lett 2014;104.
[8] Zhang H, Ma YG, Wan Y, Rong X, Xie Z, Wang W, Dai L. Measuring the refractive index of highly crystalline monolayer $MoS_2$ with high confidence. Sci Rep-Uk 2015;5.
[9] Sorensen CM, Fischbach DJ. Patterns in Mie scattering. Opt Commun 2000;173:145–53.
[10] Berg MJ, Sorensen CM, Chakrabarti A. Patterns in Mie scattering: evolution when normalized by the Rayleigh cross section. Appl Opt 2005;44:7487–93.
[11] Guinier A, Fournet G. Small-angle scattering of X-rays. New York: Wiley; 1955.
[12] Sorensen CM, Shi D. Guinier analysis for homogeneous dielectric spheres of arbitrary size. Opt Commun 2000;178:31–6.
[13] Ferri F. Use of a charge coupled device camera for low-angle elastic light scattering. Rev Sci Instrum 1997;68:2265–74.
[14] Hinds WC, Technology Aerosol. Properties, behavior, and measurement of airborne particles. New York: John Wiley & Sons Inc.; 1999.
[15] Curtis DB, Meland B, Aycibin M, Arnold NP, Grassian VH, Young MA, Kleiber PD. A laboratory investigation of light scattering from representative components of mineral dust aerosol at a wavelength of 550 nm. J Geophys Res-Atmos 2008;113.
[16] Malitson IH. Interspecimen comparison of refractive index of fused silica. J Opt Soc Am 1965;55:1205–8.
[17] Jaggard DL, Hill C, Shorthill RW, Stuart D, Glantz M, Rosswog F, Taggart B, Hammond S. Light-scattering from particles of regular and irregular shape. Atmos Environ 1981;15:2511–19.
[18] Mishchenko MI, Travis LD, Kahn RA, West RA. Modeling phase functions for dustlike tropospheric aerosols using a shape mixture of randomly oriented polydisperse spheroids. J Geophys Res-Atmos 1997;102:16831–47.
[19] Sorensen CM, Lu N, Cai J. Fractal Cluster-Size Distribution Measurement Using Static Light-Scattering. J Colloid Interf Sci 1995;174:456–60.
[20] Sorensen CM. Q-space analysis of scattering by particles: a review. J Quant Spectrosc Radiat 2013;131:3–12.
[21] Hudson PK, Gibson ER, Young MA, Kleiber PD, Grassian VH. Coupled infrared extinction and size distribution measurements for several clay components of mineral dust aerosol. J Geophys Res-Atmos 2008;113.
[22] Wang G, Chakrabarti A, Sorensen CM. Effect of the imaginary part of the refractive index on light scattering by spheres. J Opt Soc Am A 2015;32:1231–5.
[23] Sorensen CM, Maughan JB, Moosmuller H. Spherical particle absorption over a broad range of imaginary refractive index. J Quant Spectrosc Radiat 2019;226:81–6.
[24] Sorensen CM, Maughan JB, Chakrabarti A. The partial light scattering cross section of spherical particles. J Opt Soc Am A 2017;34:681–4.
[25] Sorensen CM. Q-space analysis of scattering by dusts. J Quant Spectrosc Radiat 2013;115:93–5.
[26] Heinson YW, Maughan JB, Heinson WR, Chakrabarti A, Sorensen CM. Light scattering Q-space analysis of irregularly shaped particles. J Geophys Res-Atmos 2016;121:682–91.